Available online at www.sciencedirect.com
SCIENCE DIRECT®
Enzyme and Microbial Technology 33 (2003) 430–437
ENZYME and MICROBIAL TECHNOLOGY
www.elsevier.com/locate/enzmictec

Scale-up of affinity chromatography for purification of enzymes and other proteins

Tingyue Gu [a,*], Kuang-Hsin Hsu [a], Mei-Jywan Syu [b]

[a] *Department of Chemical Engineering, Ohio University, Athens, OH 45701, USA*
[b] *Department of Chemical Engineering, National Cheng Kung University, Tainan 70101, Taiwan, ROC*

Received 27 January 2003; accepted 8 April 2003

Corrected.

Abstract

Affinity chromatography uses biospecific binding usually between an antibody and an antigen, an enzyme and a substrate or other pairs of key-lock type of matching molecules. Due to its high selectivity, it is able to purify proteins and other macromolecules from very dilute solutions. In this work, a general rate model for affinity chromatography was used for scale-up studies. Parameters for the model were estimated from existing correlations, or from experimental results obtained on a small column with the same packing material. As an example, Affi-Gel with 4.5 μmol cm^{-3} Cibacron Blue F-3GA as immobilized ligands covalently attached to cross-linked 6% agarose was used for column packing. Cibacron Blue F-3GA was also used as a soluble ligand in the elution stage. Two separate cases were studied. One involved a bovine serum albumin solution, and the other hen egg white lysozyme solution. Satisfactory scale-up predictions were obtained for a 98.2 ml column and a 501 ml column based on a few experimental data obtained on a 7.85 ml small column.

Keywords: Affinity chromatography; Rate model; Scale-up; Parameter estimation

1. Introduction

Affinity chromatography is a powerful tool for the purification of biological macromolecules such as enzymes, antibodies, and antigens. Because it uses biospecific binding between immobilized ligands and macromolecular solutes, affinity chromatography is also regarded as biospecific adsorption. A typical affinity chromatography operation involves three stages. In the frontal adsorption stage, a feed containing a target chemical, say an enzyme, and impurities is pumped into the column. Only the target enzyme will bind strongly with the column while impurities usually do not bind or bind only non-specifically, and thus weakly, through side-effect mechanisms such as hydrophobic interaction or ion-exchange. They can be easily removed in the washing stage. The target enzyme is eluted out in the elution stage.

Trial-and-error and experience combined with a few simple and rough scale-up rules are often used for the scale-up of affinity chromatography [1]. Some of the rules were discussed by Snyder et al. [2]. The particle size, column length, and flow rate are the main parameters of these empirical or semi-empirical relationships. Kang and Ryu [3] proposed dimensional scale-up of the affinity chromatography column in the radial and axial direction for an immunoglobulin separation system. Knox and Pyper [4] did an extensive study on column overload. Martin del Valle and Galan [5] studied the kinetic and mass-transfer effects in affinity chromatography. Vunnum and Cramer [6] investigated how modulators influenced protein elution profiles in metal affinity chromatography. The simple scale-up rules, however, may be not accurate enough [1]. Instead of using these rough scale-up rules, a rate model can be used to predict chromatograms of a larger column before it is built or purchased with better accuracy. In this work, a general rate model was used for scale-up.

2. Model formulation

The following basic assumptions are needed to formulate the rate model: (1) the column is isothermal, (2) the packing particles are considered spherical and possess the same size, (3) the diffusion in the radial direction is negligible, (4) there is no convective flow inside particle macropores, (5) the packing density is even along the column length, and (6) the mass-transfer and kinetic parameters are constant.

The second-order kinetics is commonly used to describe the interactions between a macromolecule and an immobi-

* Corresponding author. Tel.: +1-740-593-1499; fax: +1-740-593-0873.
E-mail address: gu@ohio.edu (T. Gu).

0141-0229/$ – see front matter © 2003 Elsevier Inc. All rights reserved.
doi:10.1016/S0141-0229(03)00141-8

Nomenclature

A	dimensionless column holdup area for a breakthrough curve
b	constant in Langmuir isotherm
Bi	Biot number for mass-transfer
C_0	feed concentration of a solute, max $\{C_f(t)\}$ (mol l^{-1})
C_b	concentration of a solute in the bulk-fluid phase (mol l^{-1})
c_b	C_b/C_0
C_f	feed concentration profile of a component (mol l^{-1})
C_p	concentration of a solute in the stagnant-fluid phase inside particle macropores (mol l^{-1})
C^∞	adsorption saturation capacity based on unit volume of particle skeleton (mol l^{-1})
C_p^*	concentration of a solute in the solid phase of particles based on unit volume of particle skeleton (mol l^{-1})
c_p	C_p/C_0
c_p^*	C_p^*/C_0
c^∞	C^∞/C_0
d	diameter of a molecule (Å)
d_c	inner diameter of a column (cm)
d_p	macropore diameter of a particle
D_b	axial dispersion coefficient (m^2 s^{-1})
D_m	intraparticle molecular diffusivity (m^2 s^{-1})
D_p	effective diffusivity in particle macropores (m^2 s^{-1})
Da^a	Damköhler number for adsorption
Da^d	Damköhler number for desorption
F^{ex}	size exclusion factor of a solute
k	film mass-transfer coefficient of a solute (m s^{-1})
k_a	adsorption rate constant
k_d	desorption rate constant
L	column length (cm)
M	molecular weight of a solute
Ns	number of components
Pe_L	Peclet number of axial dispersion for a solute
Q	mobile phase volumetric flow rate (m^3 s^{-1})
R	radial coordinate for a particle in cylindrical coordinate system
Re	Reynolds number
R_p	particle radius (m)
r	R/R_p
Sc	Schmidt number
Sh	Sherwood number
t	dimensional time ($t = 0$ is the moment a sample enters a column) (s)
t_0	retention time of a very small molecule (s)
t_d	retention time of completely excluded large molecules, e.g. blue dextran (s)
v	interstitial velocity (m s^{-1})
V_{e0}	elution volume at retention time t_0 (l)
V_{ed}	elution volume at retention time t_d (l)
z	Z/L
Z	column axial coordinate in cylindrical coordinate system

Greek letters

ε_b	bed void volume fraction
ε_p	particle porosity
ε_p^a	accessible particle porosityl
η	dimensionless group
λ	ratio of the solute molecular diameter to the pore diameter
μ	mobile phase viscosity (Pa s)
ρ	density of solvent (kg m^{-3})
τ	dimensionless time
τ_{imp}	dimensionless time duration for a rectangular pulse of a feed
τ_{tor}	pore tortuosity
ξ	dimensionless constant

Subscript

i	component i

Superscript

*	concentration of a solute in the solid of particles

lized affinity ligand,

$$P_i + L \underset{k_{di}}{\overset{k_{ai}}{\rightleftarrows}} P_i L \tag{1}$$

where P_i represents component i (a macromolecule in the mobile phase) and L is the immobilized ligand. The rate equation for Eq. (1) is as follows:

$$\frac{\partial C_{pi}^*}{\partial t} = k_{ai} C_{pi} \left(C_i^\infty - \sum_{j=1}^{Ns} C_{pj}^* \right) - k_{di} C_{pi}^* \tag{2}$$

If the reaction rates are relatively large compared to the mass-transfer rates, then instant adsorption/desorption equilibrium can be assumed. Both sides of Eq. (2) can be set to zero, which subsequently gives the Langmuir isotherm with the Langmuir equilibrium constant $b_i = k_{ai}/k_{di}$ for component i.

Using dimensionless groups $Da_i^a = L(k_{ai}C_{0i})/v$ and $Da_i^d = Lk_{di}/v$ that are defined as the Damköhler numbers for adsorption and desorption, respectively, Eq. (2) can be nondimensionalized as follows:

$$\frac{\partial c_{pi}^*}{\partial \tau} = Da_i^a c_{pi} \left(c_i^\infty - \sum_{j=1}^{Ns} \frac{C_{0j}}{C_{0i}} c_{pj}^* \right) - Da_i^d c_{pi}^* \tag{3}$$

Among various methods for elution, an inhibitor or an inexpensive soluble ligand can be used in the mobile phase for the elution stage. A binding reaction in the bulk-fluid and the stagnant fluid inside macropores of the particles between macromolecule P (component 1) and soluble ligand I (component 2) typically follows the second-order kinetics,

$$P + I \underset{k_{d2}}{\overset{k_{a2}}{\rightleftarrows}} PI \tag{4}$$

where k_{a2} and k_{d2} are the adsorption and desorption constants for P and I, and PI (component 3) denotes the complex formed from the binding of P and I. For affinity chromatography involving only one kind of macromolecule in specific binding, Eq. (1) can be rewritten as,

$$P + L \underset{k_{d1}}{\overset{k_{a1}}{\rightleftarrows}} PL \tag{5}$$

In some cases, large molecules such as P and PL cause the size exclusion effect that may not be negligible [7]. Therefore, in the model used in this work, an accessible macropore volume fraction for component i, ε_{pi}^{a}, is used to define a size exclusion factor F_i^{ex} such that $\varepsilon_{pi}^{a} = F_i^{ex}\varepsilon_p$. The F_i^{ex} value is between zero and one.

The general rate model can be written as follows:

(1) Bulk-fluid phase governing equation:

$$-D_{bi}\frac{\partial^2 C_{bi}}{\partial Z^2} + v\frac{\partial C_{bi}}{\partial Z} + \frac{\partial C_{bi}}{\partial t} + \frac{3k_i(1-\varepsilon_b)}{\varepsilon_b R_p}(C_{bi} - C_{pi,R=R_p}) - f(i)(k_{a2}C_{b1}C_{b2} - k_{d2}C_{b3}) = 0 \tag{6}$$

where $f(i) = -1$ is for components 1 and 2 ($i = 1, 2$), and $f(i) = 1$ is for component 3 ($i = 3$).

(2) Particle phase governing equation:

$$g(i)(1-\varepsilon_p)\frac{\partial C_{pi}^*}{\partial t} + \varepsilon_{pi}^{a}\frac{\partial C_{pi}}{\partial t} - \varepsilon_{pi}^{a}D_{pi}\left[\frac{1}{R^2}\frac{\partial}{\partial R}\left(R^2\frac{\partial C_{pi}}{\partial R}\right)\right] - f(i)\varepsilon_{pi}^{a}(k_{a2}C_{p1}C_{p2} - k_{d2}C_{p3}) = 0 \tag{7}$$

$$\frac{\partial C_{p1}^*}{\partial t} = k_{a1}C_{p1}(C_1^{\infty} - C_{p1}^*) - k_{d1}C_{p1}^* \tag{8}$$

in which $g(i) = 1$ for $i = 1$, and $g(i) = 0$ for $i = 2$ and 3 (i.e. only component 1 binds with the immobilized ligand). In Eqs. (6) and (7), the $f(i)$ terms are automatically zero before the elution stage because there is no soluble ligand in the feed causing C_{b2}, C_{b3}, C_{p2} and C_{p3} to be zero. In Eq. (8), C_{p1}^* represents concentration $[PL]$. Using the following dimensionless groups,

$$c_{bi} = \frac{C_{bi}}{C_{0i}}, \quad c_{pi} = \frac{C_{pi}}{C_{0i}}, \quad c_{pi}^* = \frac{C_{pi}^*}{C_{0i}}, \quad c_1^{\infty} = \frac{C_1^{\infty}}{C_{01}},$$
$$r = \frac{R}{R_p}, \quad z = \frac{Z}{L}, \quad Pe_{Li} = \frac{vL}{D_{bi}}, \quad Bi_i = \frac{k_i R_p}{\varepsilon_{pi}^{a} D_{pi}},$$
$$\eta_i = \frac{\varepsilon_{pi}^{a} D_{pi} L}{R_p^2 v}, \quad \xi_i = \frac{3Bi_i\eta_i(1-\varepsilon_b)}{\varepsilon_b}, \quad \tau = \frac{vt}{L},$$
$$Da_1^{a} = \frac{L(k_{a1}C_{01})}{v}, \quad Da_1^{d} = \frac{Lk_{d1}}{v},$$
$$Da_2^{a} = \frac{L(k_{a2}C_{02})}{v}, \quad Da_2^{d} = \frac{Lk_{d2}}{v}$$

Eqs. (6)–(8) can be transformed into dimensionless forms as follows:

$$-\frac{1}{Pe_{Li}}\frac{\partial^2 c_{bi}}{\partial z^2} + \frac{\partial c_{bi}}{\partial z} + \frac{\partial c_{bi}}{\partial \tau} + \xi_i(c_{bi} - c_{pi,r=1}) - f(i)\left(Da_2^{a}c_{b1}\frac{C_{01}}{C_{0i}}c_{b2} - Da_2^{d}\frac{C_{03}}{C_{0i}}c_{b3}\right) = 0 \tag{9}$$

$$g(i)(1-\varepsilon_p)\frac{\partial}{\partial\tau}c_{pi}^* + \varepsilon_{pi}^{a}\frac{\partial c_{pi}}{\partial\tau} - f(i)\varepsilon_{pi}^{a}\left(Da_2^{a}c_{p1}\frac{C_{01}}{C_{0i}}c_{p2} - Da_2^{d}\frac{C_{03}}{C_{0i}}c_{p3}\right) - \eta_i\left[\frac{1}{r^2}\frac{\partial}{\partial r}\left(r^2\frac{\partial c_{pi}}{\partial r}\right)\right] = 0 \tag{10}$$

$$\frac{\partial c_{p1}^*}{\partial\tau} = Da_1^{a}c_{p1}(c_1^{\infty} - c_{p1}^*) - Da_1^{d}c_{p1}^* \tag{11}$$

Note that C_{03} is replaced by C_{01} for the nondimensionalization of the concentrations of component 3 such that $C_{b3} = c_{b3}C_{01}$ and $C_{p3} = c_{p3}C_{01}$ since C_{03} is unknown before simulation.

The following initial and boundary conditions are needed for the model:

- *Initial conditions*: At $\tau = 0$, $c_{bi} = c_{bi}(0, z) = 0$, $c_{pi} = c_{pi}(0, r, z) = 0$.
- *Boundary conditions*: At $z = 0$, $\partial c_{bi}/\partial z = Pe_{Li}[c_{bi} - C_{fi}(\tau)/C_{0i}]$; and at $z = 1$, $\partial c_{bi}/\partial z = 0$; at $r = 0$, $\partial c_{pi}/\partial r = 0$; and at $r = 1$, $\partial c_{pi}/r = Bi_i(c_{bi} - c_{pi,r=1})$.

$C_{fi}(\tau)$ is the feed concentration profile of component i. $C_{fi}(\tau)/C_{0i} = 0$ is for all the three components except in the following dimensionless time periods: (a) during the frontal adsorption (sample loading) stage ($0 \le \tau \le \tau_{imp}$) in which $C_{f1}(\tau)/C_{01} = 1$ and, (b) during the elution stage with a soluble ligand solution feed ($\tau \ge \tau_{shift}$) in which $C_{f2}(\tau)/C_{02} = 1$. If there is no soluble ligand used in elution, $C_{f2}(\tau)/C_{02} = 0$. The $\tau_{imp} \le \tau \le \tau_{shift}$ period is the washing period in which there is no protein or soluble ligand in the mobile phase.

The model above was solved numerically. The finite element method was used for the discretization of Eq. (9), and the orthogonal collocation method for Eq. (10). The resultant ODE (Ordinary Differential Equation) system was solved using an ODE solver called VODE by Brown et al. [8].

3. Parameter estimation

Parameters for the model may be divided into the following three types. Physical dimensions such as column length and diameter can be easily measured with precision. Binding parameters, bed void volume fraction, and particle porosity are not readily available. A few experiments are needed to obtain these estimations. Mass-transfer coefficients can be obtained by using existing correlations. For convenience, subscript i in symbols was omitted in this section since parameter estimation must be carried out for each individual component.

3.1. Bed void fraction and particle porosity

The bed void fraction (ε_b) can be obtained from experimental data according to the following relationship [7],

$$t_d = \frac{L}{v} = \frac{0.25\pi d_c^2 L \varepsilon_b}{Q} \tag{12}$$

where t_d is the retention time of completely excluded molecules (such as blue dextran), v is calculated using Eq. (13):

$$v = \frac{4Q}{\pi d_c^2 \varepsilon_b} \tag{13}$$

The ε_p value can be calculated using Eq. (14) from the retention time of a nonbinding solute (t_0) whose molecular weight is smaller than the lower exclusion limit of the porous particle [7]:

$$t_d = \frac{t_0}{1 + (1 - \varepsilon_b)(\varepsilon_p/\varepsilon_b)} \tag{14}$$

Since the elution volume is more stable than the retention time for a solute in different runs for low-pressure systems, it is used instead of retention time. Eqs. (12) and (14) are rewritten as:

$$V_{ed} = t_d Q = 0.25\pi d_c^2 L \varepsilon_b \tag{15}$$

$$V_{ed} = \frac{V_{e0}}{1 + (1 - \varepsilon_b)(\varepsilon_p/\varepsilon_b)} \tag{16}$$

where V_{ed} and V_{e0} are the elution volumes corresponding to retention times t_d and t_0, respectively.

3.2. The adsorption saturation capacity (C^∞)

The classical batch adsorption method [9] can be used to obtain C^∞. Boyer and Hsu [10] studied stirred batch systems for the adsorption of several proteins on adsorbents prepared with different Cibacron Blue concentrations. However, their experimental C^∞ values were not based on the unit volume of particle skeleton, but based on the unit volume of a buffered adsorbent including particle porosity. This means their values could not be directly used in this work if particle density was not easily or accurately obtained for conversion. It was more convenient to use the so-called column method below to obtain isotherm parameters.

By varying C_0 values to get different A values, isotherm parameters C^∞ and b can be calculated using Eq. (17), assuming that there is no size exclusion effect [7],

$$A = \frac{(1 - \varepsilon_b)(1 - \varepsilon_p)((bC^\infty)/(1 + bC_0)) + (1 - \varepsilon_b)\varepsilon_p + \varepsilon_b}{\varepsilon_b} \tag{17}$$

In Eq. (17), A, the dimensionless area (dimensionless concentration multiplied by dimensionless time) above the concentration profile and below the dimensionless concentration unity line corresponds to the column holdup capacity.

3.3. The Damkölher number for adsorption

In this work, the determination of Da^a for the frontal adsorption stage was done by fitting model simulations with experimental breakthrough curves obtained from a small column. The Da^a value for the elution stage was also obtained from curve-fitting using an experimental elution profile.

3.4. The Damkölher number for desorption

The Damkölher number for desorption is defined by the following equation:

$$Da^d = \frac{Lk_d}{v} \tag{18}$$

where k_d represents the desorption rate constant. Da^d can also be obtained from Da^a by the following relationship:

$$Da^d = \frac{Da^a}{bC_0} \tag{19}$$

3.5. The Peclet number

The Peclet number can be evaluated from Eq. (20) [7]:

$$Pe_L = \frac{0.1L}{R_p \varepsilon_b} \tag{20}$$

3.6. The η number

To estimate the dimensionless constant η, which is expressed by the following equation:

$$\eta = \frac{\varepsilon_p^a D_p L}{R_p^2 v} \tag{21}$$

the intraparticle diffusivity (D_p) and the accessible particle porosity (ε_p^a) are needed. Yau et al. [11] used the following correlation to obtain D_p:

$$D_p = \frac{D_m(1 - 2.104\lambda + 2.09\lambda^3 - 0.95\lambda^5)}{\tau_{tor}} \tag{22}$$

in which $\lambda = d/d_p$. The tortuosity factor τ_{tor} varies from about 1.5 to over 10. A reasonable range for many commercial porous solids is about 2–6 [12]. d and d_p are the molecular diameter of the solute and the particle pore diameter, respectively. Larsson [13] reported that 6% cross-linking agarose supports have a pore diameter around 300 Å. If molecules are assumed spherical, d can be calculated from the following equation [14]:

$$d = 1.44M^{1/3} \tag{23}$$

where M is the molecular weight. Molecular diffusivities can be calculated using the following equation [15]:

$$D_m\ (\mathrm{cm^2\ s^{-1}}) = 2.74 \times 10^{-5} M^{-1/3} \tag{24}$$

3.7. The Biot number for mass-transfer

The evaluation of the Biot number (Bi) for mass-transfer:

$$Bi = \frac{kR_p}{\varepsilon_p^a D_p} \tag{25}$$

requires the value of the film mass-transfer coefficient k. Several correlations can be employed to obtain k in terms of the Sherwood number Sh. The following equation presented by Wilson and Geankoplis [16] seems suitable:

$$Sh = \frac{1.09(ReSc)^{1/3}}{\varepsilon_b} \quad (0.0015 < Re < 55) \tag{26}$$

in which $Sh = k(2R_p)/D_m$ and the Schmidt number $Sc = \mu/\rho D_m$. The Reynolds number in Eq. (26) is defined as $Re = (2R_p)(v\varepsilon_b)\rho/\mu$ which uses the superficial velocity $v\varepsilon_b$. Eq. (26) gives:

$$k = 0.687 v^{1/3} \left(\frac{\varepsilon_b R_p}{D_m}\right)^{-2/3} \tag{27}$$

3.8. Size-exclusion factor

The size-exclusion factor for a component (F^{ex}) can be determined from elution volumes [17]. Because lysozyme and BSA are relatively small enzymes their size-exclusion effects were not considered in this work. Thus, $F^{ex} = (\varepsilon_{pi}^a)/\varepsilon_p = 1$.

4. Materials and experimental methods

Two common enzymes were chosen as examples in two separate case studies: hen egg white lysozyme (MW 13,930) and bovine serum albumin (BSA) (MW 67,000). The adsorbent used in this work was Affi-Gel with 4.5 μmol cm^{-3} Cibacron Blue F-3GA covalently attached to cross-linked 6% agarose with an average wet particle diameter of 225 μm (Bio-Rad Laboratories, Richmond, CA). In the elution stage, Cibacron Blue F-3GA was also used as soluble ligands. It should be noted that there might be other elution methods for the adsorbent such as changing ionic strength, pH and adding chemicals that can weaken binding. The proteins and Cibacron Blue F-3GA were from Sigma Chemical Co. (St. Louis, MO). Blue dextran (FW 2,000,000) and glycine (FW 75.07) were used for determinations of t_d and t_0. They were purchased from Sigma and Fisher Scientific (Pittsburgh, PA), respectively. A 20 mM potassium phosphate, pH 7.0, buffer was prepared by mixing 20 mM solutions of mono- and dibasic potassium phosphate to obtain the required pH at 4 °C. This 20 mM buffered was present during all the three stages of affinity chromatography experiments. The washing stage used 20 mM NaCl in the buffer, and the elution stage used 2 mM Cibacron Blue F-3GA in the buffer unless otherwise specified. All chromatography experiments were conducted in a 4 °C cold room.

Three glass columns purchased from Kontes Glass Co. (Vineland, NJ) packed with different bed dimensions (10 cm × 1 cm i.d., 20 cm × 2.5 cm i.d., and 31.5 cm × 4.5 cm i.d.) were employed. Their bed volumes were 7.85, 98.2, and 501 ml, respectively. Effluent fractions were collected using a Model 2110 fraction collector from Bio-Rad. The chromatograms were plotted from the results of a concentration analysis using a Beckman DU 640 Spectrophotometer (Beckman Instrument, Fullerton, CA) against an appropriate buffer blank.

5. Results and discussion

5.1. Experimental results from the small 7.85 ml column

Elution volumes were obtained through a simple zonal (pulse) analysis using a mixture of blue dextrin and glycine on the 7.85 ml small column. Eqs. (15) and (16) were then used to calculate bed voidage and particle porosity. The results are listed in Table 1. Particle tortuosity τ_{tor} was given a typical value of 4.

Two experimental breakthrough curves were obtained on the 7.85 ml column for lysozyme with feed concentrations of 1 mg ml^{-1} and 2 mg l^{-1} at a flow rate of 0.1 ml min^{-1}, respectively. Eq. (17) was then used to calculate C^∞ and b_1 values. Their values for BSA were obtained in the same fashion. The C^∞ and b_1 values for the two proteins are shown in Table 2. It is interesting to note that the molar-based C^∞ value for BSA is considerably smaller than that for lysozyme. It is most likely because BSA is several times larger than lysozyme in molecular size. Thus, the accessibility of immobilized ligands for BSA may be hampered by its larger size.

Table 1
Parameter values of the small affinity chromatography bed

ε_b	ε_p	L (cm)	d_c (cm)	V_b (cm^3)	R_p (mm)
0.41	0.58	10	1	7.85	0.1125

Table 2
Langmuir isotherm parameters

Parameters	Lysozyme	BSA
C^{∞} (M)	4.41×10^{-3}	4.81×10^{-4}
b_1 (M^{-1})	1.18×10^{6}	1.42×10^{6}

One of the two breakthrough curves used to calculate C^{∞} and b_1 values for lysozyme, i.e. the $C_{0i} = 1\,\mathrm{mg\,ml^{-1}}$ curve was fitted with the model by adjusting the Da_1^{d} value as shown in the frontal adsorption part of Fig. 1. Da_1^{a} was calculated from the Da_1^{d} value and the b_1 value using Eq. (19). Because the soluble ligands used for elution were the same as the immobilized ligands in this work, it was somewhat reasonable to assume that b_2 could take the b_1 value assuming that immobilized ligands had the same affinity with solutes as free ligands in the mobile phase. The Da_2^{a} value could then be obtained from curve-fitting of an elution stage profile using the general rate model together with the Da_2^{d} value which was related to the Da_2^{a} value based on Eq. (19) once the b_2 value became known. Results from parameter sensitivity analysis showed that Da_2^{d} is quite insensitive. Fig. 1 shows

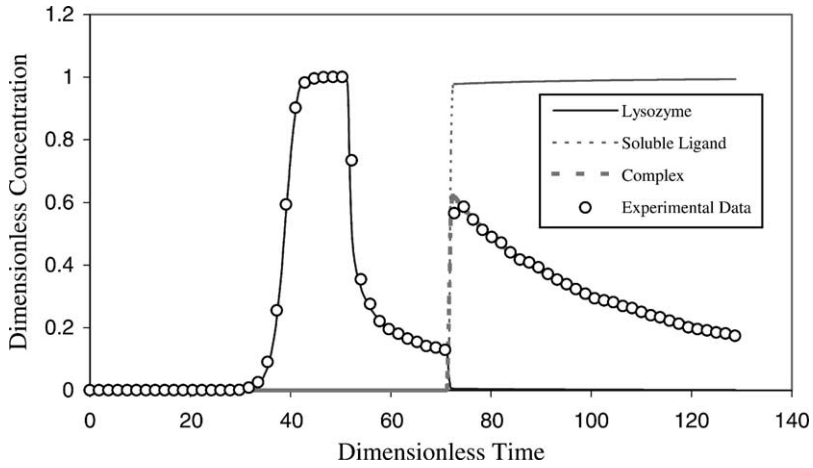

Fig. 1. Fitting of experimental data points with model calculated results for lysozyme on the small 7.85 ml column at 0.1 ml $\mathrm{min^{-1}}$.

Table 3
Parameter values used in Fig. 1

Parameters	General data	Lysozyme ($i = 1$)	Cibacron Blue ($i = 2$)	Complex ($i = 3$)	Comment
L (cm)	10				
d_c (cm)	1				
V_b (cm^3)	7.85				
R_p (mm)	0.1125				Vendor Assigned
τ_{tor}	4				
ε_b	0.41				Table 1
ε_p	0.58				Table 1
d_p (Å)	300				[13]
Q ($\mathrm{ml\,min^{-1}}$)	0.1				
v ($\mathrm{cm\,min^{-1}}$)	0.311				Eq. (13)
τ_{imp}	50				
τ_{shift}	70				
τ_{max}	130				
M_i		13930	772	14702	
C_{0i} (M)		7.18×10^{-5}	0.002	7.18×10^{-5}	
d_i (Å)		34.65	13.21	35.28	Eq. (23)
λ_i		0.115	0.044	0.118	
D_{mi} ($\mathrm{cm^2\,min^{-1}}$)		6.83×10^{-5}	1.79×10^{-4}	6.71×10^{-5}	Eq. (24)
D_{pi} ($\mathrm{cm^2\,min^{-1}}$)		1.30×10^{-5}	4.48×10^{-5}	1.27×10^{-5}	Eq. (22)
k_i ($\mathrm{cm\,min^{-1}}$)		0.028	0.057	0.028	Eq. (27)
C_i^{∞} (M)		4.41×10^{-3}	0	0	Table 2
Da_i^{a}		1.828	55.71	0	
Da_i^{d}		0.022	0.024	0	Eq. (19)
$Pe_{\mathrm{L}i}$		217.0	217.0	217.0	Eq. (20)
η_i		1.911	6.000	1.866	Eq. (21)
Bi_i		42.02	25.46	42.51	Eq. (25)

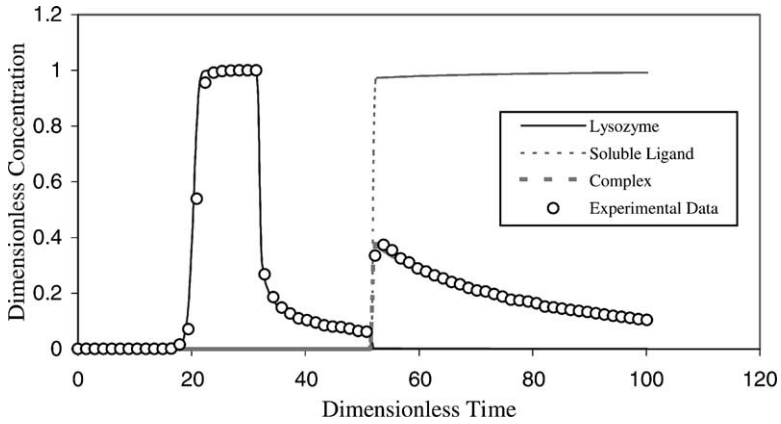

Fig. 2. Comparison between experimental results and model predictions for lysozymeon on the 98.2 ml column at 1 ml min^{-1}.

the curve-fitting results of frontal adsorption, washing and elution stages. Parameter values used for Fig. 1 are given in Table 3. In Table 3, τ_{shift} denotes dimensionless time when the elution stage starts and τ_{max} denotes the dimensionless time when model calculation is terminated. The difference between τ_{shift} and τ_{imp} is the dimensionless time duration of the washing stage. In Fig. 1, at $\tau = 50$, lysozyme feeding stopped and was followed by a buffer washing stage until $\tau = 70$ when the soluble ligand (Cibacron Blue F-3GA) solution was introduced to start the elution stage. After a delay,

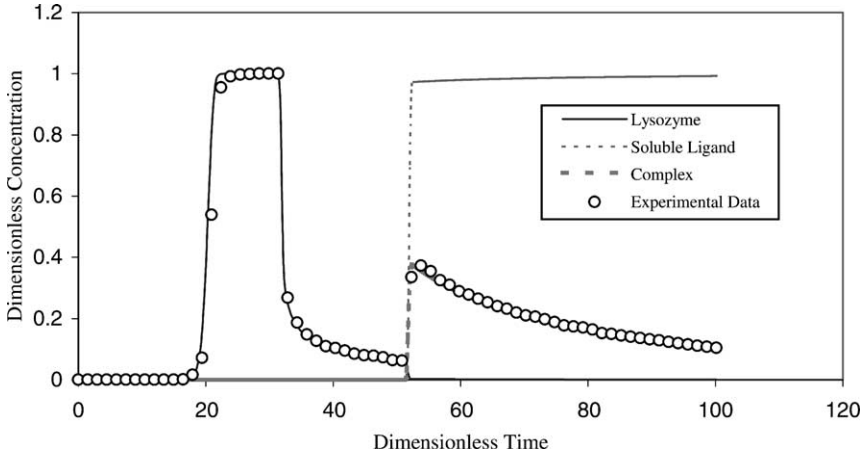

Fig. 3. Comparison between experimental results and model predictions for lysozyme on the 501 ml column at 1 ml min^{-1}.

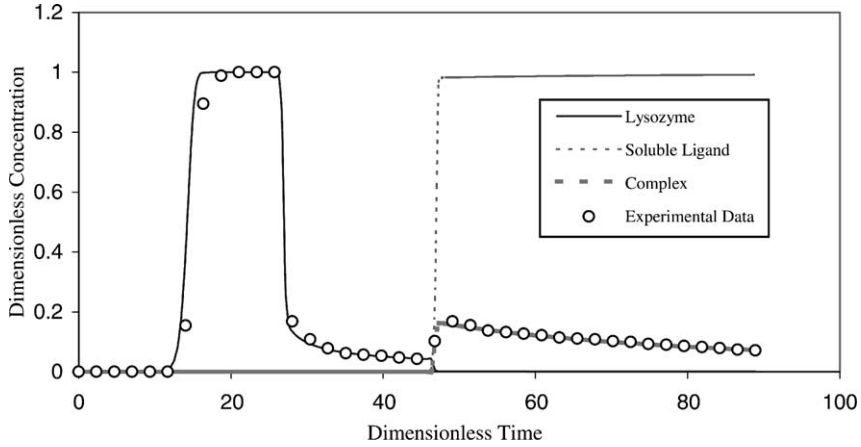

Fig. 4. Comparison between experimental results and model predictions for lysozyme on the 501 ml column at 8 ml min^{-1}.

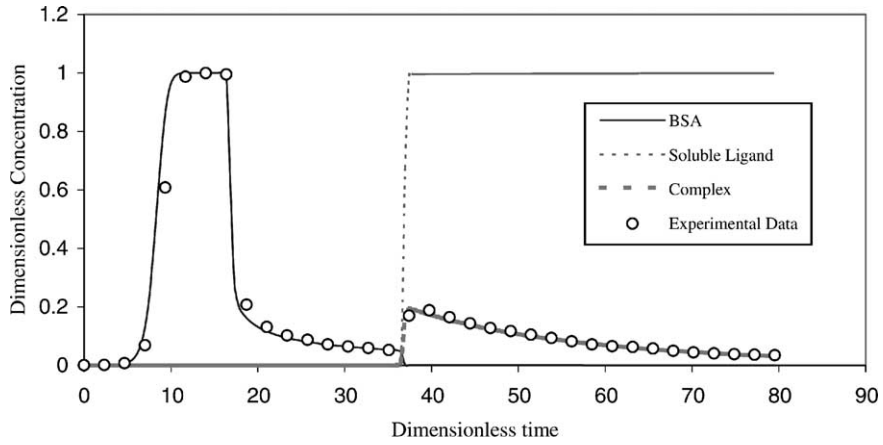

Fig. 5. Comparison between experimental results and model predictions for BSA on the 501 ml column at 8 ml min^{-1}.

the sharp soluble ligand mobile phase breakthrough curve (like a step-change) and the elution peak both appeared.

5.2. Scale-up predictions

With the parameters obtained from the small 7.85 ml column, scale-up predictions were made for lysozyme separation on the 98.2 ml column and the 501 ml column. Their bed volumes are 12.5 and 63.8 times that of the 7.85 ml column, respectively. Figs. 2–4 show the comparisons of predicted concentration profiles with experimental data points at different operating conditions. The results are surprisingly good. Similar results were obtained for BSA on the 501 ml column as shown in Fig. 5.

6. Conclusions

This work demonstrated that the general rate model predicted the concentration profiles for several runs using lysozyme and BSA on the 98.2 and 501 ml columns under different operating conditions very well. The concentration profiles of the frontal adsorption, washing, and elution stages could be predicted without a posteriori experimental data from the two columns. The rate model and the parameter estimation protocol used in this study can be used for the scale-up of affinity chromatography using soluble ligands for elution. Only a couple of experimental runs are needed on a small column in order to obtain the model input parameters that cannot be estimated using existing correlations. The Windows executable version of the simulation software used in this work is available free of charge to any researchers by contacting the corresponding author.

References

[1] Arnold FH, Blanch HW, Wilke CR. Analysis of affinity separations I: predicting the performance of affinity adsorbers. Chem Eng J Biochem Eng J 1985;30:b9–23.
[2] Snyder LR, Glejch JL, Kirkland JJ. Practical HPLC method development. New York: Wiley; 1988.
[3] Kang KA, Ryu DDY. Studies on scale-up parameters of an immunoglobulin separation system using protein A affinity chromatography. Biotechnol Prog 1991;7:205–12.
[4] Knox JH, Pyper HM. Framework for maximizing throughput in preparative liquid-chromatography. J Chromatogr 1986;363:1–30.
[5] Martin del Valle EM, Galan MA. Specific and nonspecific adsorption in affinity chromatography. Part II. Kinetic and mass transfer studies. Ind Eng Chem Res 2001;40:377–83.
[6] Vunnum S, Cramer S. IMAC: nonlinear elution chromatography of proteins. Biotech Bioeng 1997;54:373–90.
[7] Gu T. Mathematical modeling and scale-up of liquid chromatography. Berlin: Springer; 1995.
[8] Brown PN, Byrne GD, Hindmarsh AC. VODE: a variable coefficient ODE solver. SIAM J Sci Stat Comput 1989;10:1038–51.
[9] Skidmore GL, Horstmann BJ, Chase HA. Modeling single-component protein adsorption to the cation exchanger S Sepharose FF. J Chromatogr 1990;498:113–28.
[10] Boyer PM, Hsu JT. Effects of ligand concentration on protein adsorption in dye-ligand adsorbents. Chem Eng Sci 1992;47:241–51.
[11] Yau WW, Kirkland JJ, Bly DD. Modern size exclusion liquid chromatography. New York: Wiley; 1979.
[12] Satterfield C. Mass transfer in heterogeneous catalysis. Cambridge, MA: MIT Press; 1970.
[13] Larsson PO. Support materials for affinity chromatography. In: Kline T, editor. Handbook of affinity chromatography. New York: Marcel Dekker; 1993.
[14] Gu T, Zheng Y. A study of the scale-up of reversed-phase liquid chromatography. Sep Purif Technol 1999;15:41–58.
[15] Polson A. Some aspects of diffusion in solution and a definition of a colloidal particle. J Phys Colloid Chem 1950;54:649–58.
[16] Wilson EJ, Geankoplis CJ. Liquid mass transfer at very low Reynolds numbers in packed beds. Ind Eng Chem Fundam 1966;5:9–17.
[17] Li Z, Gu Y, Gu T. Mathematical modeling and scale-up of size exclusion chromatography. Biochem Eng J 1998;2:145–55.